A Three-degree-of-freedom Parallel Manipulator for Concentrated Solar Power Towers: Modeling, Simulation and Design

Ashitava Ghosal[1, a), b)] and R B Ashith Shyam[2, c)]

[1] *Professor, Robotics and Design Lab, Department of Mechanical Engineering, Indian Institute of Science, Bangalore, 560012, India*
[2] *Research Scholar, Robotics and Design Lab. Department of Mechanical Engineering, Indian Institute of Science, Bangalore, 560012, India.*
[a)] *Corresponding author: asitava@mecheng.iisc.ernet.in*
[b)] *http://www.mecheng.iisc.ernet.in/users/asitava*
[c)] *shyamashi@gmail.com*

Abstract. There is an increased thrust to harvest solar energy in India to meet increasing energy requirements and to minimize imported fossil fuels. In a solar power tower system, an array of tracking mirrors or heliostats are used to concentrate the incident solar energy on an elevated stationary receiver and then the thermal energy converted to electricity using a heat engine. The conventional method of tracking are the Azimuth-Elevation (Az-El) or Target-Aligned (T-A) mount. In both the cases, the mirror is rotated about two mutually perpendicular axes and is supported at the center using a pedestal which is fixed to the ground. In this paper, a three degree-of-freedom parallel manipulator, namely the 3-RPS, is proposed for tracking the sun in a solar power tower system. We present modeling, simulation and design of the 3-RPS parallel manipulator and show its advantages over conventional Az-El and T- A mounts. The 3-RPS manipulator consists of three rotary (R), three prismatic (P) and three spherical (S) joints and the mirror assembly is mounted at three points in contrast to the Az-El and T-A mounts. The kinematic equations for sun tracking are derived for the 3-RPS manipulator and from the simulations, we obtain the range of motion of the rotary, prismatic and spherical joints. Since the mirror assembly is mounted at three points, the wind load and self-weight are distributed and as a consequence, the deflections due to loading are smaller than in conventional mounts. It is shown that the weight of the supporting structure is between 15% and 65% less than that of conventional systems. Hence, even though one additional actuator is used, the larger area mirrors can be used and costs can be reduced.

INTRODUCTION

The growth of concentrating solar power (CSP) began in the 1980's but it gradually stopped towards mid 1990's. Then after a brief hiatus, it picked up again after 2005. The International Energy Agency (IEA) has predicted that the global CSP electricity generation is projected to grow to 4,700 TWh per year by 2050.The Solar Two in Barstow, California and the Planta Solar 10 in Sanlucar la Mayor, Spain are representatives of this technology [1]. The solar electric generation systems (SEGS) are the largest solar energy generating facility in the world. It consists of nine solar power plants in California's Mojave desert

India gets around 300 days of sunshine a year of which the daily average solar energy varies from 4 to 7 kWh/m^2 and direct normal irradiance between 1.4 to 2.0 KWh/m^2. The amount of solar power that can be generated (using photo-voltaic and/or CSP) is more than 500,000 TWh per year of electricity, assuming 10% conversion efficiency [2]. Hence there is an increased thrust to harvest solar energy in India with a target of 20GW of solar generated electricity by 2022. This includes energy harvested using photo-voltaic and from linear fresnel, parabolic dishes and troughs and central receiver (CR or solar power tower) systems. In CR systems, an array of tracking mirrors or heliostats are used to concentrate the solar energy on an elevated stationary receiver. This energy is used to run a heat engine to produce electricity and some of the energy is stored using molten salts. Steam based Rankine cycle or Brayton cycle is the most commonly used thermodynamic cycle for this operation. Some of the advantages of such a system over other approaches are high operating temperature and thus higher thermal efficiency and with storage power generation during night [3]. The thermal energy can also be used as process steam for industrial applications [4]. The disadvantages of CR systems are that the design of the structure, mirrors and drives and controller for accurate tracking of the sun can be expensive especially in presence of wind loading and other disturbances.

The conventional methods of tracking are the Azimuth-Elevation (Az-El) or Target-Aligned (T-A or spinning-elevation) mount [5] [6]. In both the cases, the mirror is rotated about two mutually perpendicular axes and is supported at the center using a pedestal which is fixed to the ground. During wind gusts, such centrally supported systems deflect and go beyond the slope error limit of 2 mrad [3]. In order to minimize the deflection, heavy backing material need to be used and cost of the heliostat increases considerably with its size. In reference [7], the use of a three degree of freedom parallel manipulator, called the 3-RPS manipulator (R-revolute, P-prismatic, S-spherical joints), is presented for use as a heliostat for CR systems. It was shown that for a given mirror size, the 3-RPS manipulator requires considerably less backing structural material as compared to Az-El or T-A mounting and thus the overall cost of the 3-RPS system is expected to be smaller. It was shown that the 3-RPS heliostat becomes more economical when larger mirrors are used. Although there is an extra motor required to track the sun, the 3-RPS manipulator is better than the conventional methods if the mirror area per actuator criteria is taken into consideration. In this paper, we build on the kinematics and structural analysis results in reference [7] . The main contributions of this work are: a) modeling of the joints to obtain their ranges and thus enable appropriate choice of the rotary (R) and spherical (S) joints, b) optimization of the location of the connection points in the top and bottom platform of the 3-RPS system to meet a structural deflection criterion of 2 mrad or less, and c) optimization of the stroke length in the prismatic joints.

This paper is organized as follows: In section 2 we present modeling and derivation of the kinematic equations for sun tracking. We present models for the spherical joints which help in obtaining the range of motion of the spherical joints. Section 2 also presents representative simulation results and the range of motion of the joints in the 3-RPS manipulator. In section 3, we present the finite element modeling of the top moving platform and we present supporting structure design approach which minimizes the weight for a chosen maximum deflection of 2 mrad and for a chosen size of the mirror. In section 4, we use the simulation results for preliminary design of the 3-RPS manipulator for sun tracking. Finally we present the conclusions and challenges ahead in section 5.

MODELING AND SIMULATION OF THE 3-RPS MANIPULATOR

The 3-RPS manipulator is a three degree-of-freedom parallel manipulator. The principle motions are rotations about X and Y axes and translation along Z axis [8]. The manipulator consists of three rotary (R), three prismatic (P) and three spherical (S) joints (see Fig. 1). The mirror assembly is mounted at the top and the different orientations of the mirror required to track the sun at various time instants are achieved by actuating the prismatic joints in a controlled manner. The points S_1, S_2 and S_3 at the top and R_1, R_2 and R_3 at the bottom form equilateral triangles of circum-radius r_p and r_b respectively. The axis of all the rotary joints lies on the plane of the bottom equilateral triangle. If a co-ordinate system is placed at the rotary joint with its z axis coinciding with the axis of the rotary joint, then the Denavit-Hartenberg (D-H) [9] parameters of a R-P-S leg can be written as in Table 1.

TABLE 1. D-H parameters of a R-P-S leg

i	α_{i-1}	a_{i-1}	d_i	θ_i
1	0	0	0	θ_1
2	-π/2	0	l_1	0

where θ_1 is the angle the leg makes with the vertical and l_1 is the translation at the prismatic joint.The basic kinematic equations of the 3-RPS manipulator were originally developed in [10] and its application as a heliostat was presented in reference [7]. For completeness, it is reproduced here in brief.

Let O represents the origin of the global co-ordinate system (*X-Y-Z*) where *OX*, *OY* and *OZ* points towards the local East, local north and zenith directions respectively (see Fig. 1). Also let O_1 and *G* represent the origin of the base (x_b-y_b-z_b) and mirror (x_m-y_m-z_m) co-ordinate systems respectively. The receiver, R, is located at [a, b, c] ^{T} with respect to global co-ordinate system. In this analysis, the center line of the receiver tower and the *OZ* axis coincides with each other (or a=0, b=0) and the height of the receiver tower from the ground is known (65 m is used in our study). The manipulator location in the field is specified by radius R_d and angle ψ with respect to *OX* axis. The orientation of the manipulator is specified an angle γ which is the angle between *OX* and O_1x_b axis. The incident solar radiation from the sun is represented by $\overrightarrow{GS}$, the reflected ray from the mirror by $\overrightarrow{GR}$ and the normal to the mirror by $\overrightarrow{GN}$.

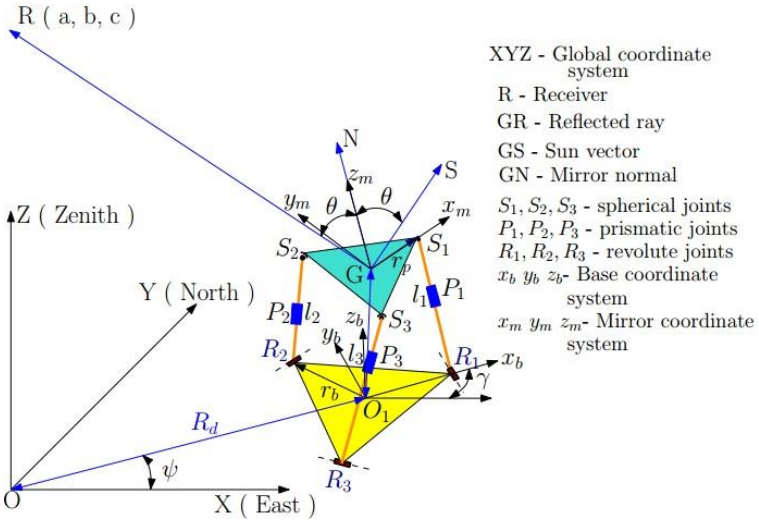

FIGURE 1. Schematic of a 3-RPS manipulator

According to the laws of refection, at any instant of time:

- The incident ray, the reflected ray and the normal should lie on the same plane
- The angle of incidence and the angle of reflection should be the same.

The vector $\overrightarrow{GS}$ can be found out by knowing the latitude and longitude of a location on the surface of earth, day of the year and time. Since only the rotational capabilities about X and Y are required for tracking the sun, the translation along Z axis is assumed to be constant. Thus the co-ordinate of origin G with respect to base co-ordinate system is given by $[x_G, y_G, z_G]^T$ where z_G is a constant (typically height of the heliostat). The homogeneous transformation matrix, $[T]_{4x4}$ which relates the base co-ordinate system (x_b-y_b-z_b) to the mirror co-ordinate system (x_m-y_m-z_m) is given by equation (1)

$$[T] = \begin{bmatrix} n_1 & o_1 & a_1 & x_G \\ n_2 & o_2 & a_2 & y_G \\ n_3 & o_3 & a_3 & z_G \\ 0 & 0 & 0 & 1 \end{bmatrix} \quad (1)$$

where a_1, a_2 and a_3 are the direction cosines of the mirror normal $\overrightarrow{GN}$. The unit vector representing the mirror normal (or the angle bisector) is given by equation (2)

$$\overrightarrow{GN} = \frac{\overrightarrow{GS} + \overrightarrow{GR}}{||\overrightarrow{GS} + \overrightarrow{GR}||} \quad (2)$$

The constraint equations in any transformation matrix are given by

$$n \cdot n = o \cdot o = 1 \quad (3)$$

$$n \cdot a = n \cdot o = o \cdot a = 0 \quad (4)$$

The three rotary joints constraint the motion of the legs of the 3-RPS manipulator in the planes defined by $y_b = 0$, and $y_b = \pm\sqrt{3}$. This introduces additional three constraints [10] given by

$$y_G + n_2 r_p = 0 \quad (5)$$

$$n_2 = o_1 \quad (6)$$

$$x_G = 0.5\, r_p\, (n_1 - o_2) \quad (7)$$

The above equations are solved using Matlab [11] function *fsolve* for the unknowns in ***[T]*** at every instant of time. Once ***[T]*** is found out, the stroke required for the prismatic joints for any orientation of the mirror can be found out as follows:

The stroke of the prismatic joint, l_i, i=1,2,3 is a function of several variables such as the location of the heliostat in a field, the location of the receiver tower, the angle γ, day of the year and the circum-radius of the bottom and top

equilateral triangles r_b and r_p. To obtain l_i extensive computations are required to account for each of the mentioned variables. To simplify the analysis and search, intelligent guesses are made as follows:

- The change in l_i is maximum for the heliostats nearest to the receiver tower – R_d = 50m assumed.
- The key dates for the motion of the sun are the summer solstice, winter solstice, March equinox and the September equinox and only these four days are considered for the analysis and search.

The distance R_iS_i or the leg length l_i, i=1, 2, 3 is given by

$$l_i = \| \boldsymbol{[T]} * GS_i - O_1R_i \| \quad (8)$$

where ***[T]*** the homogeneous transformation matrix. The value of z_G chosen for the analysis is 3m and ***[T]*** is found out from 8 a.m. to 5 p.m. at an interval of 10 minutes. A search is carried out in Matlab to find out the values of γ and r_b which ensures the stroke to be less than a desired quantity (700 mm chosen in our case). The analysis is done for Bangalore, India (Latitude 12^0 58' 13" N and Longitude 77^0 33' 37" E). Figure 2 shows the plot of the variation of azimuth and elevation angles of the sun vector. Figure 3 gives the variation of leg length with time of the 3-RPS manipulator and Figure 4 gives the variation of rotary joint angle with time.

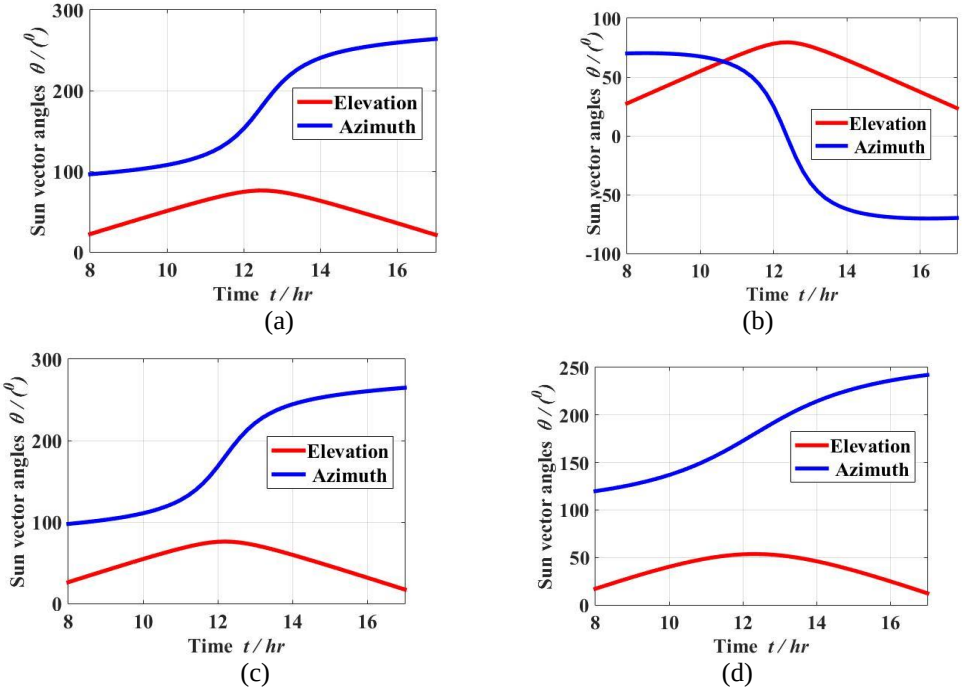

FIGURE 2. Azimuth and Elevation angles of the sun for (a) March equinox (b) Summer solstice (c) September equinox (4) Winter solstice

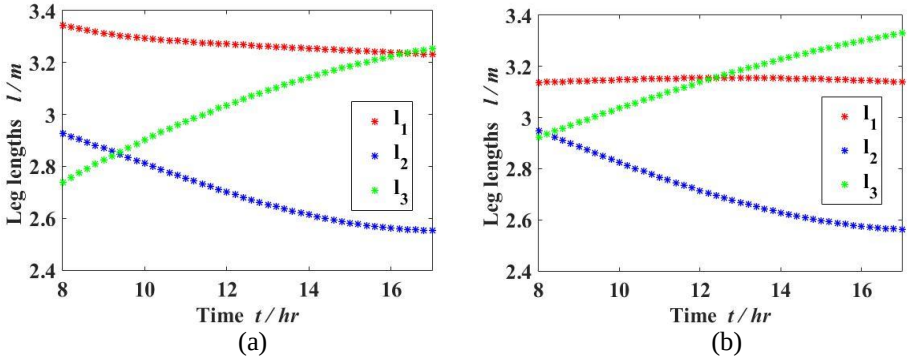

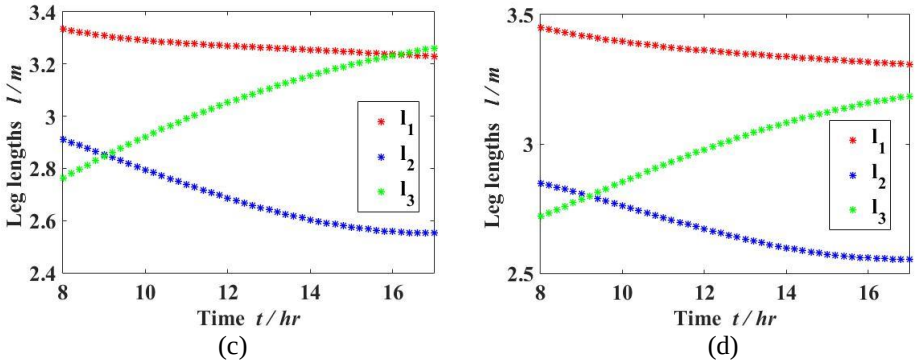

FIGURE 3. Plot of leg lengths for (a) March equinox (b) Summer solstice (c) September equinox (4) Winter solstice

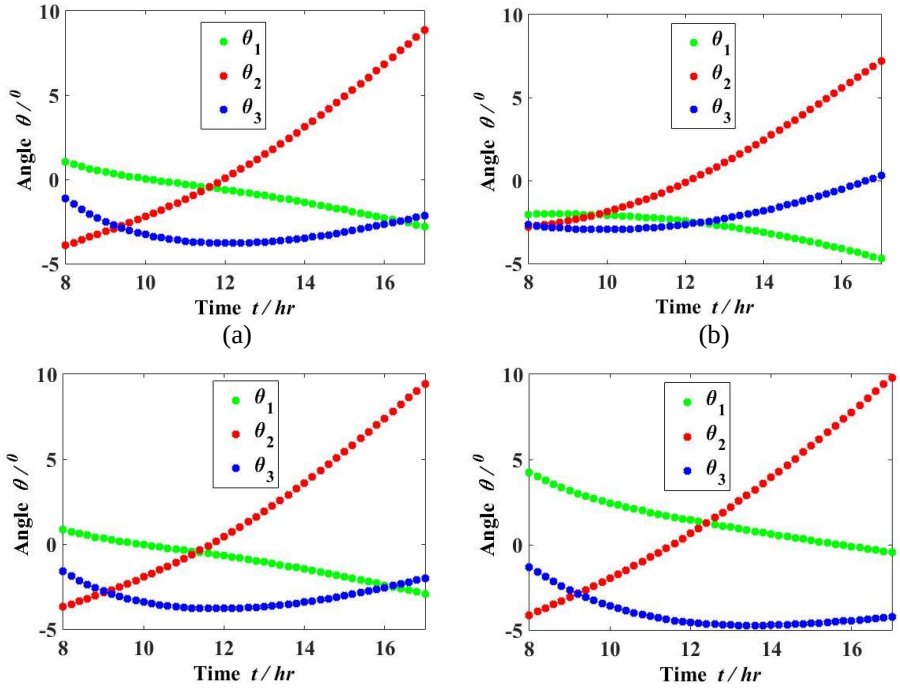

FIGURE 4. Variation of the rotary joint angle for (a) March equinox (b) Summer solstice (c) September equinox (4) Winter solstice

The spherical joints can be modeled as three mutually perpendicular revolute joints [9]. From the base of the leg, a set of four consecutive rotations, namely rotation of the rotary joint and the Z-Y-X (or 321) rotation of the spherical joint, gives the mirror coordinate system (x_m-y_m-z_m). Figure 5 shows the co-ordinate system associated with a spherical joint and the resulting D-H table of the spherical joint is shown in Table 2 [12].

TABLE 2. D-H parameters of the spherical joint

i	α_{i-1}	a_{i-1}	d_i	θ_i
3	0	0	0	θ_{s1}
4	-π/2	0	0	$\theta_{s2} + \pi/2$
5	π/2	0	0	$\theta_{s3} + \pi/2$
6	-π/2	0	0	-π/2

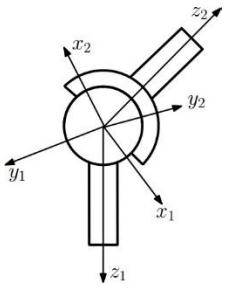

FIGURE 5. Schematic of a spherical joint

The three rotations (Z-Y-X rotation) is found out by using the following algorithm:

If $r_{31} \neq \pm 1$, then

θ_{s2} = Atan2 [$-r_{31}$, $\pm\sqrt{{r_{32}}^2 + {r_{33}}^2}$]

θ_{s1} = Atan2 [r_{21}/cos (θ_{s2}) , r_{11}/cos (θ_{s2})]

θ_{s3} = Atan2 [r_{32}/cos (θ_{s2}) , r_{33}/cos (θ_{s2})]

If $r_{31} = 1$, then

$\theta_{s2} = -\pi/2$, $\theta_{s1} = 0$, θ_{s3} = Atan2 [$-r_{12}$, $-r_{13}$]

If $r_{31} = -1$, then

$\theta_{s2} = \pi/2$, $\theta_{s1} = 0$, θ_{s3} = Atan2 [r_{12} , r_{13}]

where $r_{ij,}$ i, j = 1, 2, 3 represents the row and column of the ***[T]*** matrix found out earlier. From the above algorithm, for each angle, a pair of solutions is obtained. The obtained solutions were verified by using a MSC ADAMS [13] model. Figure 6 shows the angular (Z-Y-X) motion of the spherical joint for leg 1 and leg 2 for tracking the sun on March 20 for $R_d = 300$ and $\psi = 30^0$. The Z rotation in a spherical joint can be between 0 and 360^0 and is not shown.

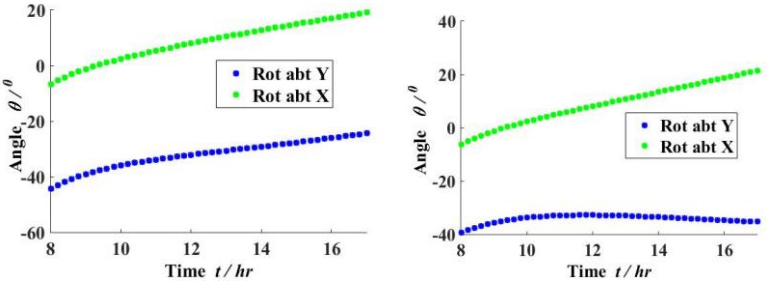

FIGURE 6. Variation of the spherical joint angles with time

FINITE ELEMENT MODELING OF THE MIRROR AND SUPPORT FRAME ASSEMBLY.

A CAD model of the mirror and the support frame is made in SolidWorks [14] and imported to ANSYS Workbench [15] for finite element analysis. The two main aspects analyzed are whether the displacement at any place exceeds the slope error criteria of 2 mrad and the stress generated due to gravity and wind loading. A wind speed, *v*, of 10 m/s is considered to be safe operating limit and the whole structure should withstand short duration gusty winds up to 22 m/s [16] and be brought back to its stowed position if winds exceed this value. The uniform wind load (*P*) on the surface of the mirror is calculated by using the equation $P = 0.5 C_d \rho v^2 FoS$, where C_d=1.18 is the drag coefficient, ρ is the density of air assumed to be 1.25 kg/m^3 and FoS = 2, is the factor of safety. A number of support frame topologies are tried out to arrive at the lightest possible one and the support points at the top defined by r_p is varied to satisfy the slope error criteria. Table 2 gives the comparison of weight and deflection for Az-El and 3-RPS mounts and it can be seen that the weight of the support structure is 15% - 65% less for 3-RPS than the Az-El method.

TABLE 3. Comparison of weight and deflection for Az-El and 3-RPS

Wind speed (v) (m/s)	*Frame (m x m)*	*Az-El*			*3-RPS*		
		Max. Deformation (mm)	*Stress (Pa)*	*Weight of frame (kg)*	*Max. Deformation (mm)*	*Stress (Pa)*	*Weight of frame (kg)*
10	2 x 2	1.8862	3.6076E+07	20.94	1.93	4.156E+07	15
	3 x 3	2.6489	3.9829E+07	53.53	2.45	2.595E+07	45
	5 x 5	4.736	2.9694E+07	356.97	4.90	2.889E+07	198
22	2 x 2	1.8872	4.6809E+07	41	1.82	5.728 E+07	30
	3 x 3	2.874	4.3612E+07	181.17	2.66	5.518 E+07	93
	5 x 5	4.7281	2.5648E+07	1332.54	4.92	5.119E+07	535

DESIGN OF A 3-RPS HELIOSTAT

This work is towards prototyping a heliostat with 2m x 2m mirror. The design of the 3-RPS heliostat involves kinematic and structural analysis, choice of actuators and drives, and finally sensors and controller. In this section, we present the values obtained for kinematic and structural parameters only, viz., r_p, γ, r_b, stroke, range of the spherical joint motion and range of rotary joint motion based on extensive simulations for heliostats located in a field where R_d varies from 50m to 300m in steps of 5m and ψ varies from 0 to 350^0 in steps of 10^0. We present parameter values for the assumed values of mirror size (2 m x 2m), height of receiver (65 m), z_G of 3m etc. – the approach can be easily used for other geometries and arrangements of heliostats.

- From the finite element analysis, the optimum value of r_p is found out to be 500 mm and the lightest support frame found out is as shown in Fig. 7.

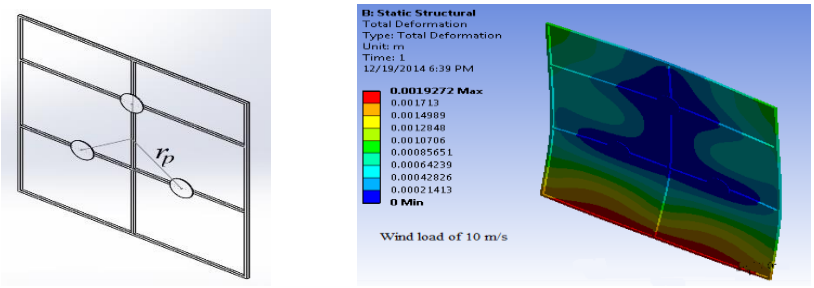

(a) (b)

FIGURE 7. (a) Support frame and (b) structural analysis of a 2m x 2m mirror for a wind loading of 10 m/s

- The optimum values of the angle γ is [66,71,75,80,85,86,86,87,89,90,91, 93,94,94,97,101,106, 110, 114,119,120,120,120,120,120,120,120,120,120, 120, 80, 66, 60, 53, 58, 62] for every 10^0 change of ψ from 0^0 to 350^0.
- The value of r_b which ensures a stroke of less than 700mm is found to be 360 mm.
- For March 20 and for a location specified by $R_d = 300$, $\psi = 30^0$ and $\gamma = 80^0$, the strokes of the three P joints obtained are 112.2 mm, 374.1mm and 514.9 mm.
- For the same parameters, the ranges of the spherical joint motion for the three legs are as shown in Table 3.

TABLE 4. Range of rotation of the spherical joints

Leg 1		Leg 2		Leg 3	
Y rotation range	X rotation range	Y rotation range	X rotation range	Y rotation range	X rotation range
-44.27^0 - -24.35^0	-6.76^0-19.02^0	-39.34^0 - -32.81^0	-6.25^0 – 21.34^0	-42.11^0 - -24.98^0	-6.52^0 – 19.12^0

- The corresponding range of motion of the rotary joints measured from the vertical are obtained as -2.80^0 – 0.89^0, -3.75^0 – 8.86^0 and -1.47^0 - -3.78^0 for leg 1, leg 2 and leg 3 respectively.

CONCLUSIONS AND CHALLENGES AHEAD

This work presents modeling, simulation and design of a 3-RPS parallel manipulator and shows that it can be used as a heliostat. Kinematic simulation results are used to obtain and optimize the stroke of the linear actuators and mathematical models of spherical joints are used to obtain the range of motion of the spherical joints. Maximum stroke of the translation (P) joint is found to be less than 700 mm for r_b = 360mm and r_p = 500mm. Range of motion of spherical joint is $\pm 70^0$ and range of motion of R joint is less than $\pm 10^0$ from vertical. Weight of the support structure required to withstand wind load for deflection less than 2 mrad is 15% - 65% less for 3-RPS when compared to Az-El method.

These can be used to select cost effective commercially available actuators and joints. Also the finite element analysis of the supporting structure is used to obtain the lightest possible support frame that can withstand wind loading and self-weight keeping in view the deflection constraints. The modeling and simulations help in designing a cost-effective 3-RPS parallel manipulator for sun tracking.

One of the main challenges that we look forward to is to make a prototype and test in real environmental conditions. This will validate our approach and can be used to determine required modifications.

ACKNOWLEDGMENTS

This research is based upon work supported in part by the Solar Energy Research Institute for India and the U.S. (SERIIUS) funded jointly by the U.S. Department of Energy subcontract DE AC36-08G028308 (Office of Science, Office of Basic Energy Sciences, and Energy Efficiency and Renewable Energy, Solar Energy Technology Program, with support from the Office of International Affairs) and the Government of India subcontract IUSSTF/JCERDC-SERIIUS/2012 dated 22nd Nov. 2012.

REFERENCES

1. C. E. Tyner, *Concentrating Solar Power in 2001: An IEA/SolarPACES Summary of Present Status and Future Prospects*. (SolarPACES, 2001).
2. A. Sharma, Renewable and Sustainable Energy Reviews **15** (4), 1767-1776 (2011).
3. L. Vant-Hull, in *Concentrating solar power technology: principles, developments and applications, Woodhead Publishing, Cambridge, UK*, edited by K. L. a. W. Stein (Woodhead Publishing, Cambridge, UK, 2012), pp. 240-283.
4. A. Haberle, in *Concentrating solar power technology: Principles, developments and applications* edited by K. Lovegrove and W. Stein (Woodhead Publishing, Cambridge, UK, 2012), pp. 602-619.
5. H. Ries and M. Schubnell, Solar Energy Materials **21** (2), 213-217 (1990).
6. R. Zaibel, E. Dagan, J. Karni and H. Ries, Solar Energy Materials and Solar Cells **37** (2), 191-202 (1995).
7. R. B. Ashith Shyam and A. Ghosal, Chinese Journal of Mechanical Engineering **28** (4), 793-800 (2015).
8. R. A. Srivatsan, S. Bandyopadhyay and A. Ghosal, Mechanism and Machine Theory **69**, 127-141 (2013).
9. A. Ghosal, *Robotics: fundamental concepts and analysis*, 5 ed. (Oxford University Press, New Delhi, India, 2006).
10. K.-M. Lee and D. K. Shah, Robotics and Automation, IEEE Journal of **4** (3), 354-360 (1988).
11. MATLAB, in *Inc., Natick, MA* (1998), Vol. 5, pp. 333.
12. S. Shah, S. Saha and J. Dutt, Journal of Computational and Nonlinear Dynamics **7** (2), 021006 (2012).
13. M. ADAMS and C. Documentation, in *Software Corporation* (2005).
14. SolidWorks, Concord, MA (2002).
15. ANSYSWorkbench, (Cannonsburg, PA, 2011), Vol. v.14.
16. J. A. Peterka, Z. Tan, B. Bienkiewicz and J. Cermak, NASA STI/Recon Technical Report N **89**, 22179 (1988).